

# Rashba spin-orbit coupling effects in armchair graphene nanoribbons

Cite as: AIP Conference Proceedings **1653**, 020088 (2015); <https://doi.org/10.1063/1.4914279>  
Published Online: 13 April 2015

S. Prabhakar, R. Melnik, and A. Sebetci



View Online



Export Citation

## ARTICLES YOU MAY BE INTERESTED IN

[Spin-orbit force in graphene with Rashba spin-orbit coupling](#)

Journal of Applied Physics **111**, 07B330 (2012); <https://doi.org/10.1063/1.3678488>

[Electronic analog of the electro-optic modulator](#)

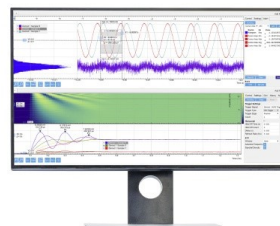
Applied Physics Letters **56**, 665 (1990); <https://doi.org/10.1063/1.102730>

[Third nearest neighbor parameterized tight binding model for graphene nano-ribbons](#)

AIP Advances **7**, 075212 (2017); <https://doi.org/10.1063/1.4994771>

## Challenge us.

What are your needs for  
periodic signal detection?



Zurich  
Instruments



# Rashba Spin-orbit Coupling Effects in Armchair Graphene Nanoribbons

S. Prabhakar<sup>1</sup>, R. Melnik<sup>1, a)</sup> and A. Sebetci<sup>2</sup>

<sup>1</sup>*The MS2Discovery Interdisciplinary Research Institute, M2NeT Laboratory, Wilfrid Laurier University, Waterloo, ON, N2L 3C5*

<sup>2</sup>*Department of Mechanical Engineering, Mevlana University, 42003 Konya, Turkey*  
<sup>a)</sup> *rmelnik@wlu.ca*

**Abstract.** We study the influence of the Rashba spin-orbit coupling effects on the electronic properties of armchair graphene nanoribbons (GNRs). By utilizing both analytical and numerical schemes, we show that the finite width of the graphene nanoribbon breaks its energy spectrum into an infinite number of bands. By considering the Rashba spin-orbit coupling term as a perturbation, we show that zero energy bands between electron and hole states at Dirac points are lifted into a finite bandgap.

**Keywords:** Armchair graphene, bandstructure, spin-orbit coupling, Finite Element Method.

**PACS:** 71.38.-k, 72.20.Dp, 78.70.Ck, 63.22.-m

## INTRODUCTION

Graphene has attracted much interest due to the design of next generation electronic devices. It possesses unique bandstructure and physical properties [1-3]. Several observed unique properties such as the half integer quantum Hall effect, non-zero Berry phase, as well as measurement of conductivity of electrons in the electronic devices made from graphene, lead to novel applications in carbon based nanoelectronics [1,2,4]. The experimental data observed by the quantum Hall effect measurement technique suggest that the one atom thick graphene sheet demonstrates the properties of a two dimensional system that does not contain any bandgap at Dirac points[5]. However, it is possible to induce a bandgap for the application of graphene in semiconductor and optoelectronic devices in areas including spintronics and photonics. In this paper, we show that the Rashba spin-orbit coupling induces a bandgap of approximately 20 meV at Dirac points.

## THEORETICAL MODEL

In the continuum limit, by expanding the momentum close to the K point in the Brillouin zone, the total Hamiltonian of electrons in graphene can be read as:  
 $H = H_0 + H_{\text{int}} + H_{\text{so}}$  [2,6]. Here  $H_0$  is the Hamiltonian for  $\pi$  electrons at the K point,  $H_{\text{int}}$  and  $H_{\text{so}}$  are the intrinsic and the Rashba spin-orbit couplings. Mathematically, these components of the total Hamiltonian can be written as [6,7]:

$$H_0 = v_F (\sigma_x p_x + \sigma_y p_y), \quad (1)$$

$$H_{\text{int}} = \Delta_{\text{int}} \sigma_z s_z, \quad (2)$$

$$H_{so} = \lambda_R (\sigma_x s_y - \sigma_y s_x). \quad (3)$$

For armchair graphene nanowire [8], we assume  $(H_0 + H_{\text{int}})\psi = \varepsilon\psi$ , where  $\psi(r) = \exp(iky) (\phi_A \ \phi_B)^T$ . Here  $\phi_A$  and  $\phi_B$  are the wavefunctions of electrons on the sublattices  $A$  and  $B$  respectively of graphene. Thus, based on (1) and (2), we can derive the following two coupled equations:

$$-i\hbar v_F (\partial_x + k_y) \phi_B = (\varepsilon - \Delta_{\text{int}}) \phi_A, \quad (4)$$

$$-i\hbar v_F (\partial_x - k_y) \phi_A = (\varepsilon - \Delta_{\text{int}}) \phi_B. \quad (5)$$

We apply operator  $-i\hbar v_F (\partial_x - k_y)$  to Eq. (4) and by using Eq. (5), we write the resulting second order partial differential equation as:

$$(\hbar v_F)^2 (k_y^2 - \partial_x^2) \phi_B = (\varepsilon^2 - \Delta_{\text{int}}^2) \phi_B, \quad (6)$$

Its solution is

$$\phi_B = A_1 \exp(ik_n x) + B_1 \exp(-ik_n x), \quad (7)$$

where  $A_1$  and  $B_1$  are arbitrary constants. In a similar way, the wavefunction of electrons in graphene at another Dirac point ( $K'$ ) can be written as

$$\phi_B' = C_1 \exp(ik_n x) + D_1 \exp(-ik_n x), \quad (8)$$

with arbitrary constants  $C_1$  and  $D_1$ . Thus, energy eigenvalues of (6) can be written as

$$\varepsilon_{n\pm}^0 = \pm \sqrt{(\hbar v_F)^2 (k_y^2 + k_n^2) + \Delta_{\text{int}}^2}, \quad (9)$$

where  $k_n$  can be found by utilizing boundary condition  $\psi_A|_{x=0} = \psi_B|_{x=0} = \psi_A|_{x=L} = \psi_B|_{x=L} = 0$ . For graphene with armchair edge, we must admix the wavefunctions at valleys  $K$  and  $K'$  in order to find the coefficients  $A_1$  and  $B_1$ . Thus we write the boundary conditions of (7) and (8) as:

$$\phi_\mu(0) + \phi_\mu'(0) = 0, \quad (10)$$

$$\exp(iKL)\phi_\mu(L) + \exp(iK'L)\phi_\mu'(L) = 0 \quad (11)$$

with  $\mu = A, B$ . The above equations can be satisfied with the choice  $B_1 = C_1 = 0$  and  $A_1 = -D_1$ . We normalized the wavefunctions on each sublattices  $A$  and  $B$  separately [8]:

$$\int dr [\psi_\mu(r)^2 + |\psi'_\mu(r)|^2] = 1/2 \quad (12)$$

Hence, we write the normalized wavefunctions at the Dirac points  $K$  and  $K'$  as:

$$\phi_B = \frac{1}{2\varepsilon\sqrt{L}}(k_n - ik_y)\exp(ik_n x), \quad (13)$$

$$\phi_B = \frac{1}{2\sqrt{L}}\exp(ik_n x), \quad (14)$$

$$\phi'_A = \frac{1}{2\varepsilon\sqrt{L}}(k_n - ik_y)\exp(-ik_n x), \quad (15)$$

$$\phi'_B = -\frac{1}{2\sqrt{L}}\exp(-ik_n x). \quad (16)$$

Also we write  $k_n$  as:

$$k_n = \frac{n\pi}{L} - \frac{4\pi}{3\sqrt{3}a}, \quad (17)$$

where  $a$  is the lattice constant of hexagonal graphene. At this point, we use Eq. (3) as a perturbation term of (9) and write the energy spectrum of electron-hole like states of graphene nanowire:

$$\varepsilon_{n\pm} = \pm\sqrt{(\hbar v_F)^2(k_y^2 + k_n^2) + \Delta_{\text{int}}^2 + 4\lambda_R^2}. \quad (18)$$

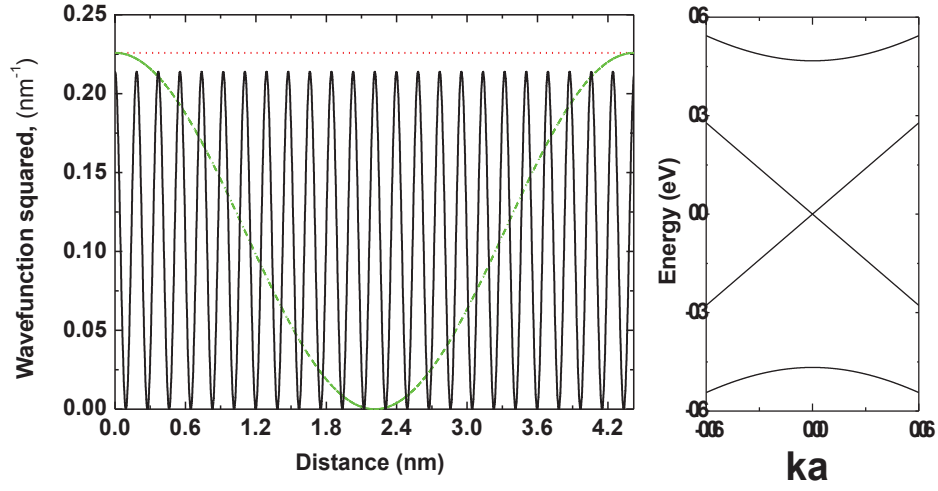


**FIGURE 1.** (a) Wavefunctions squared vs distance in an armchair GNR without intrinsic and spin-orbit couplings at Dirac K point ( $k_y = 0$ ). These plots are obtained from Eqs.(13) and (15) by considering  $\varphi_A = \phi_A + \phi'_A$  to admix the valleys of armchair GNR. We choose the width of the GNR as  $L = 3\sqrt{3}aN(N=6)$  (dotted line for  $n = 4N$  and dashed-dotted line for  $n = 4N + 1$ ) and  $L = \sqrt{3}a(3N + 1)$  (solid line for  $n=0$ ) to reproduce the results of Ref.[8]. (b) The bandstructures of metallic (i.e.  $L = 3\sqrt{3}aN(N=6)$ ) armchair GNR without intrinsic and spin-orbit couplings. We also choose  $v_F = 10^6 \text{ m/s}$ .

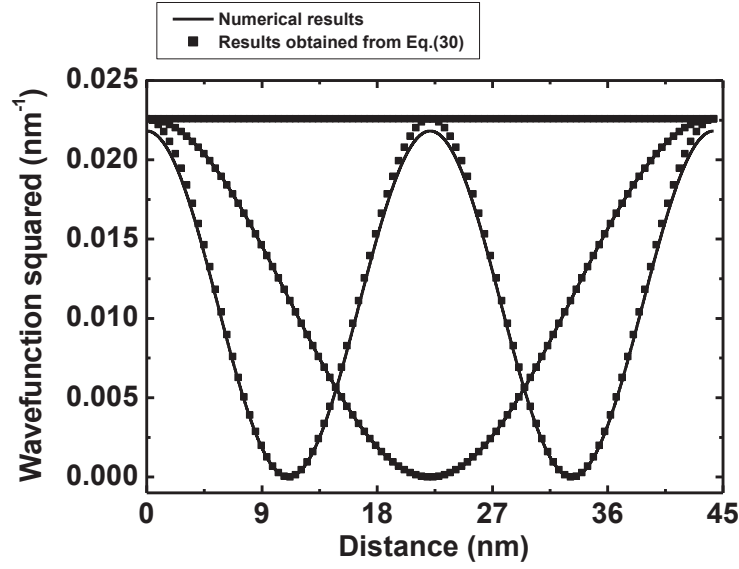


**FIGURE 2.** (a) Ground and first excited state wavefunctions squared vs distance in an armchair GNR without intrinsic and spin-orbit couplings at Dirac K point ( $k_x=0$ ). Here we consider  $L = 3\sqrt{3}aN(N = 60)$ . Note that the numerical results obtained via the exact diagonalization technique are seen to be in excellent agreement with the analytical results.

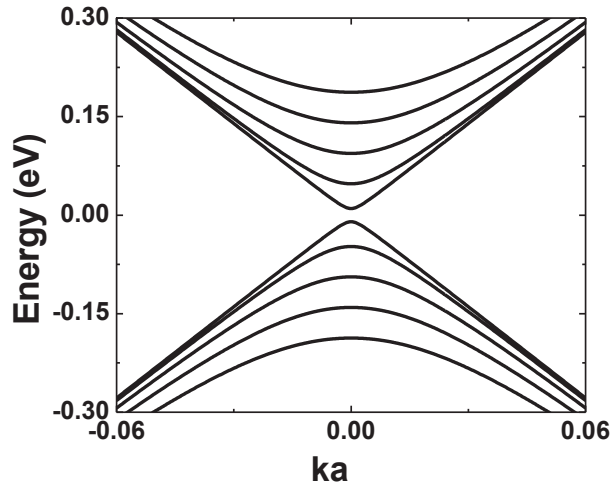


**FIGURE 3.** Spin-orbit coupling effects on the bandstructure of armchair GNR. The spin-orbit coupling effect lifts the degeneracy and opens a bandgap of approx 20meV. We choose  $L = 3\sqrt{3}aN(N = 60)$ ,  $\Delta_{int} = 0.01 \text{ meV}$ ,  $\lambda_R = 5 \text{ meV}$  and  $v_F = 10^6 \text{ m/s}$ .

## RESULTS and DISCUSSIONS

In Fig. 1 (left panel), we plot wavefunctions squared of armchair graphene vs distance at Dirac points. We find that  $n = 24$  corresponds to the lowest state that has zero energy and there is no confinement effect on the form of the wavefunction which is shown by dotted line in Fig. 1 (left panel). For  $n=25$ ,  $k_n \neq 0$  and thus we find the wavefunction in the form of confined mode which is shown by dotted line. For  $n = 0$ , the oscillations in the wavefunction can be observed that are shown by solid line in Fig. 1 (left panel). Two lowest bands of the armchair graphene nanoribbon are plotted in Fig. 1 (right panel). As can be seen, at a Dirac point, the zero bandgap energy shows the metallic behaviour. In Fig. 2, we plot the wavefunctions squared of the unconfined modes (zero energy eigenvalues) and confined modes. The analytically obtained results (squares) are seen to be in excellent agreement to the numerical values (solid lines). In Fig. 3, we plot the bandstructure of the graphene nanoribbon with armchair edge. As can be seen, at the Dirac point, the intrinsic and Rashba spin-orbit coupling terms lift the degeneracy and we find the bandgap of approximately  $20meV$  that can be utilized in the design and implementation of graphene based optoelectronic devices.

## CONCLUSIONS

To conclude, by utilizing both analytical and numerical schemes based on the Finite Element Method, we have presented the bandstructure analysis of graphene nanoribbons with the armchair edge. In the absence of spin-orbit coupling, the vanishing bandgap shows the properties of metallic behaviors in graphene. In the presence of intrinsic and the Rashba spin-orbit couplings, we have shown that the degeneracy is lifted at the Dirac point and found the bandgap of approximately  $20meV$ .

## ACKNOWLEDGMENTS

This work has been supported by NSERC and CRC programs (Canada). RM and AS are grateful to TUBITAK for its support.

## REFERENCES

1. S. Das Sarma, S. Adam, E. Hwang, and E. Rossi, [Rev. Mod. Phys.](#) 83, 407 (2011).
2. A. H. Castro Neto, F. Guinea, N. M. R. Peres, K. S. Novoselov and A. K. Geim, [Rev. Mod. Phys.](#) 81, 109 (2009).
3. S. Prabhakar, R. Melnik, L. Bonilla and J. Raynolds, [Applied Physics Letters](#) 103, 233112 (2013).
4. M. Droth and G. Burkard, [Phys. Rev. B](#) 87, 205432 (2013).
5. K. S. Novoselov, A. K. Geim, S. V. Morozov, D. Jiang, M. I. Katsnelson, I. V. Grigorieva, S. V. Dubonos, A. A. Firsov, [Nature](#) 438, 197 (2005).
6. D. Huertas-Hernando, F. Guinea and A. Brataas, [Phys. Rev. B](#) 74, 155426 (2006).
7. S. Prabhakar, R. Melnik, L. Bonilla and S. Badu, [Phys. Rev. B](#) 90, 205418 (2014).
8. L. Brey and H. A. Fertig, [Phys. Rev. B](#) 73, 235411 (2006).



# 4. INTERNATIONAL ADVANCES IN APPLIED PHYSICS & MATERIALS SCIENCE CONGRESS & EXHIBITION

24-27 April 2014 / Fethiye

## SCITEED

International Congress & Exhibition on Current  
Trends on Science & Technology Education  
24-27 April 2014 / Fethiye

